Manipulation of Airy Beams in Dynamic Parabolic Potentials

*Feng Liu, Jingwen Zhang, Wei-Ping Zhong, Milivoj R. Belić, Yu Zhang, Yanpeng Zhang, Fuli Li, and Yiqi Zhang**

The propagation of finite energy Airy beams in dynamic parabolic potentials, including uniformly moving, accelerating, and oscillating potentials, is investigated. The propagation trajectories of Airy beams are strongly affected by the dynamic potentials, but the periodic inversion of the beam remains invariant. The results may broaden the potential applications of Airy beams, and also enlighten ideas on Airy beam manipulation in nonlinear regimes.

1. Introduction

The Airy beam, which originated from the Airy wavepacket in quantum mechanics,[1] was introduced into optics by superposing an exponential function to an Airy function, to obtain a finite-energy beam.[2,3] The finite energy Airy beam possesses some unique properties including self-acceleration, nondiffraction, and self-healing.[4] It is demonstrated that Airy beams can be used for superresolution fluorescence imaging, plasmons generation, material processing, filamentation, to manipulate micro-particles, and so on.[5–8] Until now, investigations of Airy beams have been reported in nonlinear media,[9–15] Bose–Einstein condensates,[16] on the surface of a metal,[17–20] in optical fibers,[21–24] and other systems. In a word, Airy beams have attracted a lot of attention all over the world in the past few decades, and a large quantity of related literature has sprouted out. Among multitudinous research results that are about manipulation of the Airy beam behavior, external potentials feature prominently, such as the parabolic potential,[25–29] linear potential,[30] and dynamic potentials in general.[31,32]

A dynamic potential means that the potential changes with the evolution or propagation distance,[31–33] so that it can modulate the beam behavior simultaneously. A dynamic potential could be changed by the propagating beam itself, which is common occurrence in the nonlinear regime. Even though Airy beams in dynamic potentials have been reported,[31,32] their behavior in a dynamic parabolic potential has not been explored yet, to the best of our knowledge. A parabolic potential is important, because it naturally arises when strongly nonlocal nonlinearity is treated,[14,34] which conveniently reduces a nonlinear problem into a linear one. In addition, the parabolic potential plays a role of Fourier transform operator during propagation, and based on this serendipitous effect, new kinds of self-Fourier beams have been discovered.[26,27]

In this paper, we investigate the propagation behavior of Airy beams in dynamic parabolic potentials. We will tackle the following problems. As it is well known, an Airy beam will undergo periodic inversion and phase transition during propagation in a parabolic potential. The first task is to investigate whether these properties are preserved in dynamic parabolic potentials and how they are affected by the potentials. Also, we will look into the properties of trajectories of Airy beams during propagation and how they are affected by the concrete type of dynamics coming from the potentials. We believe that the results of our investigation may not only provide effective and diverse methods for linear manipulation of Airy beams, but also have enlightening ideas on the nonlinear control of such beams.

Dr. F. Liu, Dr. J. W. Zhang, Prof. Y. P. Zhang, Dr. Y. Q. Zhang
Key Laboratory for Physical Electronics and Devices of the Ministry of Education & Shaanxi Key Lab of Information Photonic Technique
School of Electronic and Information Engineering
Xi'an Jiaotong University
Xi'an 710049, China
E-mail: zhangyiqi@mail.xjtu.edu.cn

Prof. W.-P. Zhong
Department of Electronic and Information Engineering
Shunde Polytechnic
Shunde 528300, China

Prof. M. R. Belić
Science Program
Texas A&M University at Qatar
P.O. Box 23874 Doha, Qatar

Dr. Y. Zhang
Xi'an Institute of Optics and Precision Mechanics of Chinese Academy of Sciences
Xi'an, Shaanxi 710119, China

Prof. F. L. Li
Department of Applied Physics
School of Science
Xi'an Jiaotong University
Xi'an 710049, China

The ORCID identification number(s) for the author(s) of this article can be found under https://doi.org/10.1002/andp.201900584

DOI: 10.1002/andp.201900584

2. Theoretical Analysis

The paraxial propagation of a beam in a dynamic parabolic potential, is described by the dimensionless Schrödinger equation

$$i\frac{\partial\psi(x,z)}{\partial z} = -\frac{1}{2}\frac{\partial^2\psi(x,z)}{\partial x^2} + \frac{1}{2}\alpha^2[x-t(z)]^2\psi(x,z) \tag{1}$$

where x and z are the normalized transverse coordinate and the propagation distance, respectively.[12,13] Parameter α scales the width of the potential. The function $t(z)$ in Equation (1) determines the dynamic behavior of the parabolic potential. Such

 © 2020 WILEY-VCH Verlag GmbH & Co. KGaA, Weinheim

modulated potential can be achieved by appropriately changing the refractive index of the material.

We first perform Fourier transform (FT) of Equation (1), to obtain

$$i\frac{\partial\hat{\psi}(k,z)}{\partial z} = -\frac{1}{2}\alpha^2\frac{\partial^2\hat{\psi}(k,z)}{\partial k^2} - i\alpha^2 t(z)\frac{\partial\hat{\psi}(k,z)}{\partial k} + \frac{1}{2}[k^2 + \alpha^2 t^2(z)]\hat{\psi}(k,z) \tag{2}$$

where the FT is defined as

$$\hat{\psi} = \int_{-\infty}^{+\infty} \psi \exp(-ikx)dx, \quad \psi = \frac{1}{2\pi}\int_{-\infty}^{+\infty} \hat{\psi}\exp(ikx)dk$$

If the dynamic function $t(z)$ is zero (corresponding to a static parabolic potential), then Equation (2) has exactly the same form as Equation (1), when $\alpha = 1$. But when $t(z) \neq 0$, the second term and $\alpha^2 t(z)$ in the third term on the right-hand side of Equation (2) lead to different scenarios.

To change the dynamic potential into a static potential, we do a coordinate transform operation through the relations $X = x - t(z)$ and $Z = z$, and now Equation (1) is written as

$$i\frac{\partial\psi(X,Z)}{\partial Z} = -\frac{1}{2}\frac{\partial^2\psi(X,Z)}{\partial X^2} + i\frac{dt(Z)}{dZ}\frac{\partial\psi(X,Z)}{\partial X} + \frac{1}{2}\alpha^2 X^2\psi(X,Z) \tag{3}$$

As expected, the propagation trajectory of beams in such a static potential will not be affected by the dynamic function, because the "external force" in Equation (1) becomes an "inertial force" in this transformed frame, which only stretches or suppresses the beams along the transverse coordinate. Making a comparison between the second terms on the right-hand side of Equations (2) and (3), one finds that the major difference is that Equation (2) contains $t(z)$ but Equation (3) contains dt/dz. Therefore, if the beam behavior is not affected much by the dynamic function in Equation (3), it will be definitely affected in Equation (2).

Again, we perform FT of Equation (3), to find

$$i\frac{\partial\tilde{\psi}(K,Z)}{\partial Z} = -\frac{1}{2}\alpha^2\frac{\partial^2\tilde{\psi}(K,Z)}{\partial K^2} + \left(\frac{1}{2}K^2 - K\frac{dt(Z)}{dZ}\right)\tilde{\psi}(K,Z) \tag{4}$$

where now

$$\tilde{\psi} = \int_{-\infty}^{+\infty} \psi\exp(-iKX)dX, \quad \psi = \frac{1}{2\pi}\int_{-\infty}^{+\infty}\tilde{\psi}\exp(iKX)dK$$

Clearly, the dynamic function plays an "external force" in Equation (4). If one introduces $K' = K - dt(Z)/dZ$ and $h(Z) = [dt(Z)/dZ]^2$, then Equation (4) can be rewritten as

$$i\frac{\partial\tilde{\psi}(K',Z)}{\partial Z} = -\frac{1}{2}\alpha^2\frac{\partial^2\tilde{\psi}(K',Z)}{\partial K'^2} + \frac{1}{2}\left[K'^2 - h(Z)\right]\tilde{\psi}(K',Z) \tag{5}$$

If one further sets $\tilde{\psi} = \tilde{\phi}\exp[i\int \frac{1}{2}h(Z)dZ]$ and $K' = \alpha\kappa$, Equation (5) is recast into

$$i\frac{\partial\tilde{\phi}(\kappa,Z)}{\partial Z} = -\frac{1}{2}\frac{\partial^2\tilde{\phi}(\kappa,Z)}{\partial\kappa^2} + \frac{1}{2}\alpha^2\kappa^2\tilde{\phi}(\kappa,Z) \tag{6}$$

Obviously, Equation (6) has the same form as Equation (1), except for the form of the dynamic function. Both equations can have similar solutions but expressed in different spaces, real and Fourier. Also, Equations (1) and (6) indicate that localized light beams in real and Fourier spaces may share similar dynamics from a mathematical point of view, but along different paths. The solution of Equation (6) can be written as[26–28]

$$\tilde{\phi}(\kappa,Z) = \tau(\kappa,Z)\int_{-\infty}^{+\infty}\left[\tilde{\phi}(\xi,0)\exp\left(i\mathscr{P}\xi^2\right)\right]\exp(-i\mathscr{Q}\xi)d\xi \tag{7}$$

where $\mathscr{P} = \frac{\alpha}{2}\cot(\alpha Z)$, $\mathscr{Q} = \alpha\kappa\csc(\alpha Z)$, and

$$\tau(\kappa,Z) = \sqrt{-\frac{i}{2\pi}\frac{\mathscr{Q}}{\kappa}}\exp\left(i\mathscr{P}\kappa^2\right)$$

Based on Equation (7), one can obtain the solution of Equation (2), and finally the solution of Equation (1). According to Equation (7), one finds that the propagation of the beam $\tilde{\phi}(\kappa,Z)$ is equivalent to a Fourier transform (with $\mathscr{Q}$ being the frequency) of the modified beam $\tilde{\phi}(\xi,0)\exp(i\mathscr{P}\xi^2)$ at each Z.

Theoretical analysis indicates that the beam behavior in a dynamic parabolic potential can still be understood in terms of the behavior in a static parabolic potential, but with appropriate changes in the form of solutions. The propagation properties in a dynamic parabolic potential may be connected with those in a static parabolic potential, provided proper changes are introduced in the solutions in the Fourier and transformed coordinate spaces. For example, the "center of mass" of the finite energy Airy beam might follow a straight line or a parabolic curve or perform a harmonic oscillation in the transformed coordinate. But, the concrete profile of the dynamic parabolic potential will modulate the trajectory and the dynamics of the beam during propagation.

Since Airy beams have some unique properties, such as being nondiffracting, self-accelerating, and self-healing, and are of high current interest in optics, we will take Airy beams as our investigating objects. Note that the discussion can be easily extended to two-dimensional (2D) cases,[28] and also other beams,[35] for example, beams with orbital angular momentum (e.g., Hermite–Gaussian or Laguerre–Gaussian beams).

In the following text, we will investigate the propagation dynamics of Airy beams in three typical dynamic parabolic potentials. We consider the quantities dt/dz and d^2t/dz^2 which indicate the velocity and acceleration of the dynamic potential.[36] If dt/dz is a constant, then the potential moves uniformly during propagation. While if d^2t/dz^2 is constant along the propagation distance, then the potential is uniformly accelerating. We will start with the two simple cases, then discuss the oscillating case and finally, the 2D case. For uniformity in the treatment, we set $\alpha = 0.5$ throughout.

3. Uniformly Moving Parabolic Potential

We set the dynamic function as a general linear function $t(z) = \mu z + \nu$, and pick $\mu = 3$ and $\nu = 0$. So, $dt/dz = 3$ and $d^2t/dz^2 = 0$, and the potential moves uniformly with velocity $dt/dz = 3$ during propagation.

© 2020 WILEY-VCH Verlag GmbH & Co. KGaA, Weinheim

We first solve for the analytical solution with the general linear function based on the equations in Section 2, and then numerically investigate the propagation dynamics of the input beams. Although the input beams can be arbitrary, our attention here is focused only on finite-energy Airy beams, $\psi(x) = \mathrm{Ai}(x)\exp(ax)$ with $a = 0.1$. We would like to emphasize again that our analytical method is generally applicable to any input beam. While the finite-energy Airy beam is the input in Equation (1), the input in Equation (7) should be

$$\tilde{\phi}(\kappa) = \exp\left[-a(\alpha\kappa+\mu)^2\right] \times \exp\left\{\frac{a^3}{3} + \frac{i}{3}\left[(\alpha\kappa+\mu)^3 - 3a^2(\alpha\kappa+\mu)\right]\right\}$$

which is the Fourier transform of the finite-energy Airy beam. Inserting this input into Equation (7), one obtains

$$\begin{aligned}\tilde{\phi}(\kappa, Z) =& \tau(\kappa, Z)\int_{-\infty}^{+\infty} d\xi \exp(-i\mathscr{Q}\xi) \\ &\times \exp\left[-a(\alpha\xi+\mu)^2\right]\exp\left(i\mathscr{P}\xi^2\right) \\ &\times \exp\left\{\frac{a^3}{3} + \frac{i}{3}\left[(\alpha\xi+\mu)^3 - 3a^2(\alpha\xi+\mu)\right]\right\}\end{aligned}$$

Considering that

$$\int_{-\infty}^{+\infty} \exp(i\mathscr{P}\xi^2)\exp(-i\mathscr{Q}\xi)d\xi = \sqrt{i\frac{\pi}{\mathscr{P}}}\exp\left(-i\frac{\mathscr{Q}^2}{4\mathscr{P}}\right)$$

and

$$\begin{aligned}&\int_{-\infty}^{+\infty} \exp(-i\mathscr{Q}\xi)d\xi \exp\left[-a(\alpha\xi+\mu)^2\right] \\ &\times \exp\left\{\frac{a^3}{3} + \frac{i}{3}\left[(\alpha\xi+\mu)^3 - 3a^2(\alpha\xi+\mu)\right]\right\} \\ &= \frac{2\pi}{\alpha}\mathrm{Ai}\left(-\frac{\mathscr{Q}}{\alpha}\right)\exp\left(-(a-i\mu)\frac{\mathscr{Q}}{\alpha}\right)\end{aligned}$$

the solution of Equation (6) can be written as a convolution

$$\begin{aligned}\tilde{\phi}(\kappa, Z) =& \frac{\tau(\kappa, Z)}{\alpha}\sqrt{i\frac{\pi}{\mathscr{P}}}\exp\left(-i\frac{\mathscr{Q}^2}{4\mathscr{P}}\right)\circledast \\ &\left[\mathrm{Ai}\left(-\frac{\mathscr{Q}}{\alpha}\right)\exp\left(-(a-i\mu)\frac{\mathscr{Q}}{\alpha}\right)\right]\end{aligned}$$

where $\circledast$ represents the convolution operation. Therefore, the solution of Equation (4) is

$$\begin{aligned}\tilde{\psi}(K, Z) =& \frac{\tau(K, Z)}{\alpha}\exp\left(i\frac{\mu^2}{2}Z\right)\sqrt{i\frac{\pi}{\mathscr{P}}}\exp\left(-i\frac{\mathscr{Q}^2}{4\mathscr{P}}\right)\circledast \\ &\left[\mathrm{Ai}\left(-\frac{\mathscr{Q}}{\alpha}\right)\exp\left(-(a-i\mu)\frac{\mathscr{Q}}{\alpha}\right)\right]\end{aligned}$$

To find the solution of Equation (3), one takes the inverse Fourier transform of this solution,

$$\psi(X, Z) = \frac{1}{2\pi}\int_{-\infty}^{+\infty}\tilde{\psi}(K, Z)\exp(iKX)dK$$

which turns out to be

$$\begin{aligned}\psi(X, Z) =& \frac{\mathrm{Ai}(A^2+B)}{\sqrt{\cos(\alpha Z)}}\exp\left[\frac{1}{3}\left(2A^3+3AB+C^3\right)\right] \\ &\times \exp\left[\frac{i}{2}\left(-\frac{\alpha\sin(\alpha Z)}{\cos(\alpha Z)}X^2 + 2\mu X + \mu^2 Z\right)\right]\end{aligned} \quad (8)$$

where $A = \frac{i\sin(\alpha Z)}{2\alpha\cos(\alpha Z)} + C$, $B = \frac{X}{\cos(\alpha Z)} - C^2$, and $C = a - i\mu$. By replacing X with $x - \mu z - \nu$ and Z with z, one finally obtains the general solution of Equation (1) with the uniformly moving parabolic potential,

$$\begin{aligned}\psi(x, z) =& \frac{\mathrm{Ai}(A^2+B)}{\sqrt{\cos(\alpha z)}}\exp\left[\frac{1}{3}\left(2A^3+3AB+C^3\right)\right] \\ &\times \exp\left[\frac{i}{2}\left(-\frac{\alpha\sin(\alpha z)}{\cos(\alpha z)}(x-\mu z-\nu)^2\right)\right] \\ &\times \exp\left[\frac{i}{2}(2\mu x - \mu^2 z - 2\mu\nu)\right]\end{aligned} \quad (9)$$

According to Equation (9), there are singular points at $z = (2n+1)\frac{\pi}{2\alpha}$ with n being natural numbers, at which the "phase transition" happens. Obviously, the singular points are independent of the dynamic function. Since Equation (9) is invalid at $z = (2n+1)\frac{\pi}{2\alpha}$, one has to solve for the solution at these points, which is

$$\begin{aligned}\psi\left(x, z = (2n+1)\frac{\pi}{2\alpha}\right) =& -\sqrt{-i\frac{s\alpha}{2\pi}}\exp\left(i\frac{\mu^2}{2}z + \frac{C^3}{3}\right) \\ &\times \exp\left[\frac{i}{3}s^3\alpha^3(x-\mu z-\nu)^3\right] \\ &\times \exp\left[-C\alpha^2(x-\mu z-\nu)^2\right] \\ &\times \exp\left[is\left(\mu-\alpha C^2\right)(x-\mu z-\nu)\right]\end{aligned} \quad (10)$$

where $s = 1$ if n is even and $s = -1$ if n is odd. In **Figure 1**a, we display the propagation dynamics of the input finite-energy Airy beam based on the analytical results.

Now, we investigate the beam behavior numerically by solving Equations (1)–(3) successively, and the results are displayed in Figures 1b–d, respectively. In Figure 1b, the trajectory of the dynamic function $t = 3z$ is displayed by the dashed line. It is obvious that the analytical and numerical results completely agree with each other. One finds that the Airy beam propagates along a step-wise trajectory, with the center of mass following the straight dashed line. One also notes that the periodic inversion and "phase transition" (i.e., a mutual transformation between an Airy beam and a Gaussian beam) performed by the Airy beam are there, as indicated by the analytical solutions. However, the profiles of the beam in the first and second stages are different. In

 © 2020 WILEY-VCH Verlag GmbH & Co. KGaA, Weinheim

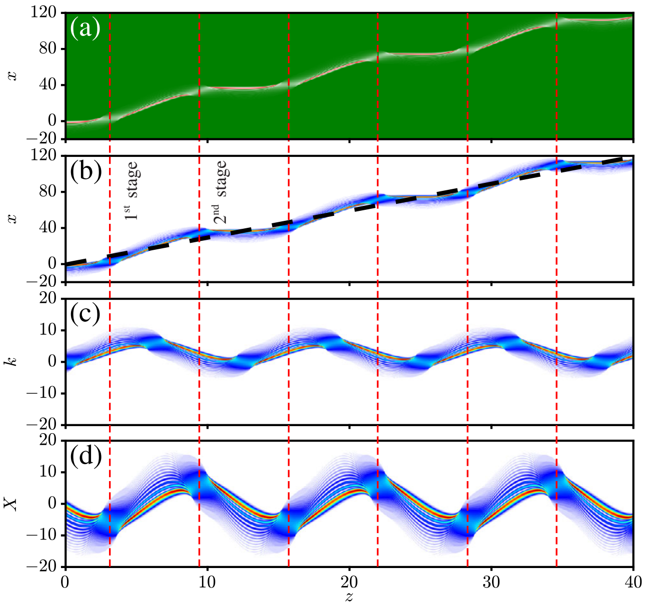

Figure 1. Propagation of a finite energy Airy beam in a uniformly moving parabolic potential $t(z) = 3z$ [represent by the dashed curve in (b)]. (a) Analytical result according to Equations (9) and (10). b–d) Numerical result in the real space, in the inverse space, and in the transformed frame, respectively. For discussion convenience, the red dashed vertical lines separate the two propagation stages.

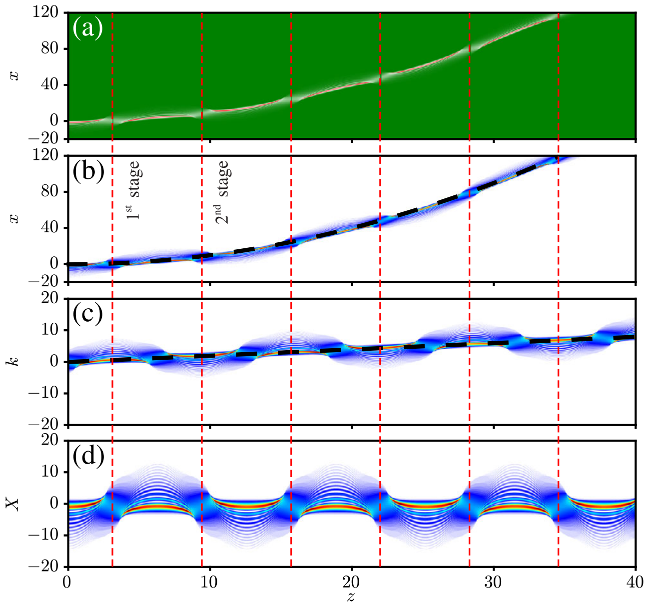

Figure 2. Propagation of a finite energy Airy beam in an accelerating parabolic potential $t(z) = 0.1z^2$. The setup is as in Figure 1.

the second stage, the barycenter of the beam remains on a quite stable level, but in the first stage the process changes sharply. The two stages do not obey centro-symmetry about the dashed line. The reason for such a phenomenon can be attributed to the parity asymmetry of the finite Airy beam. If one uses a Gaussian beam as the input in such a dynamic potential, one would find that the process is centro-symmetric about the dashed line.

It is also interesting to note that the inversion period projected onto the z coordinate does not change, which is $5\pi/4\alpha$. Such an invariance can be demonstrated from the corresponding propagation displayed in the Fourier space [Figure 1c] and in the transformed frame [Figure 1d], in which the propagation trajectories are not affected by the dynamic function. It is worth mentioning that in the transformed frame, the beam dynamics exhibits centro-symmetry about $X = 0$, which is expected.

4. Accelerating Parabolic Potential

If the dynamic potential is written as a general quadratic function, $t(z) = \mu z^2 + \nu z + \ell$ with, say, $\mu = 0.1$ and $\nu = \ell = 0$, one finds $d^2t/dz^2 = 0.2$, which is constant. Therefore, this is an accelerating parabolic potential.

Following the same procedure as in Section 3, the analytical solution with the general quadratic function can be obtained as

$$\begin{aligned}\psi(x,z) =& \frac{\mathrm{Ai}(A^2+B)}{\sqrt{\cos(\alpha z)}} \exp\left[\frac{1}{3}\left(2A^3+3AB+C^3\right)\right]\\ &\times \exp\left[\frac{i}{2}\left(-\frac{\alpha\sin(\alpha z)}{\cos(\alpha z)}\left(x-\mu z^2-\nu z-\ell\right)^2\right)\right]\\ &\times \exp\left[i(2\mu z+\nu)\left(x-\mu z^2-\nu z-\ell\right)\right]\\ &\times \exp\left[\frac{i}{2}\left(\frac{4}{3}\mu^2 z^3+2\mu\nu z^2+\nu^2 z\right)\right]\end{aligned} \tag{11}$$

with $A = \frac{i\sin(\alpha z)}{2\alpha\cos(\alpha z)} + C$, $B = \frac{x-\mu z^2-\nu z-\ell}{\cos(\alpha z)} - C^2$, and $C = a - i\nu$. At the critical points, the solution is

$$\begin{aligned}\psi\left(x, z=(2n+1)\frac{\pi}{2\alpha}\right) =& -\sqrt{-i\frac{s\alpha}{2\pi}} \exp\left(\frac{C^3}{3}\right)\\ &\times \exp\left[\frac{i}{2}\left(\frac{4}{3}\mu^2 z^3+2\mu\nu z^2+\nu^2 z\right)\right]\\ &\times \exp\left[\frac{i}{3}s^3\alpha^3(x-\mu z^2-\nu z-\ell)^3\right]\\ &\times \exp\left[-C\alpha^2(x-\mu z^2-\nu z-\ell)^2\right]\\ &\times \exp\left[is\left(2\mu z+\nu-\alpha C^2\right)(x-\mu z^2-\nu z-\ell)\right]\end{aligned} \tag{12}$$

As a check on the solution, if one sets $\mu = 0$, Equation (11) reduces to Equation (9), and Equation (12) reduces to Equation (10). The propagation dynamics based on the analytical solution is displayed **Figure 2**a. And the corresponding numerical simulations are exhibited in Figure 2b–d. In Figure 2b, the center of mass of the Airy beam propagates along an accelerating dynamic potential, which is indicated by the parabolic dashed curve. Different from the uniformly moving parabolic potential in Figure 1, the Airy beam does not exhibit explicitly the difference in the stages, except that the beam is elongated along the dashed curve. The reason is quite obvious—the inversion period projected onto the z coordinate is invariant, but the slope of the subsequent stages increases.

© 2020 WILEY-VCH Verlag GmbH & Co. KGaA, Weinheim

In the Fourier space, as shown in Figure 2c, the beam propagates along the trajectory $dt/dz = 0.2z$ (the dashed line), which is a linear function of the propagation distance z. Recall that in Figure 1c, the beam is seemingly not affected by the dynamic function in the Fourier space, because dt/dz is constant, which is invariant with the propagation distance z. As elucidated before, the beam propagation is related to $t(z)$ in the Fourier space, but is connected with dt/dz in the transformed space. Since in the transformed space, as exhibited in Figure 2d, the trajectory of the beam is affected by the dynamic function, the trajectory in the Fourier space must also be modulated by the dynamic function. One can infer that if the dynamic function obeys a cubic power law $t(z) = az^3$, then the beam in the Fourier space will propagate along a parabolic trajectory $dt/dz = 3az^2$. Numerical simulations and theoretical results confirm such a prediction (not shown). In principle, one can surely obtain mathematical verification on this prediction by doing Fourier transform on the analytical solution in Equation (13), which includes the term dt/dz.

In Section 3 and this section, the dynamic functions are polynomials, and corresponding analytical solutions are obtained. Actually, for polynomial functions, a general analytical solution can also be obtained. One can demonstrate that the corresponding solution can be written as

$$\psi(x,z) = \frac{\mathrm{Ai}(A^2+B)}{\sqrt{\cos(\alpha z)}} \exp\left[\frac{1}{3}\left(2A^3+3AB+C^3\right)\right] \times \exp\left[i\frac{dt(z)}{dz}[x-t(z)]\right] \exp\left[\frac{i}{2}\int\left(\frac{dt(z)}{dz}\right)^2 dz\right] \times \exp\left[\frac{i}{2}\left(-\frac{\alpha\sin(\alpha z)}{\cos(\alpha z)}[x-t(z)]^2\right)\right] \tag{13}$$

where $t(z)$ is the polynomial function, and $A = \frac{i\sin(\alpha z)}{2\alpha\cos(\alpha z)} + C$, $B = \frac{x-t(z)}{\cos(\alpha z)} - C^2$, and $C = a - i\frac{dt(z)}{dz}|_{z=0}$. At the critical points, the general solution turns out to be

$$\psi\left(x, z=(2n+1)\frac{\pi}{2\alpha}\right) = -\sqrt{-i\frac{s\alpha}{2\pi}} \exp\left(\frac{C^3}{3}\right) \times \exp\left[\frac{i}{2}\int\left(\frac{dt(z)}{dz}\right)^2 dz\right] \times \exp\left[\frac{i}{3}s^3\alpha^3[x-t(z)]^3 - C\alpha^2[x-t(z)]^2\right] \times \exp\left[is\left(\frac{dt(z)}{dz} - \alpha C^2\right)[x-t(z)]\right] \tag{14}$$

5. Oscillating Parabolic Potential

In this Section, we use a complex dynamic potential of the form $t(z) = \mu\sin(\nu z)$ with $\mu = 4\pi^2$ and $\nu = 4$, which harmonically oscillates during propagation. A relevant question to ask is whether then there exists an analytical solution for such a dynamic function. Unfortunately, the answer is no. The reason is that the dynamic function will automatically connect with the term $\sin(\alpha z)$ in the integral, which makes it difficult to evaluate, owing to the complex relation between $\sin(\alpha z)$ and $\sin(\nu z)$. While one can still denote a solution given up to an integral as an analytical solution, we prefer to refer to it as a numerical solution, since it can be fully investigated only numerically. The numerical results are displayed in **Figure 3**.

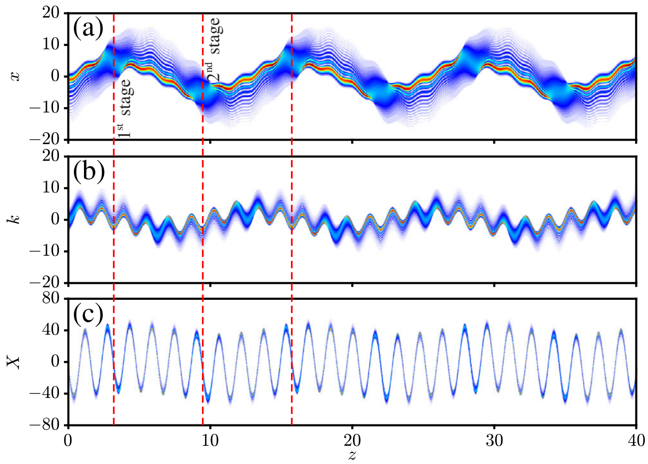

Figure 3. Propagation of a finite energy Airy beam in an oscillating parabolic potential $t(z) = 4\pi^2\sin(4z)$. The setup is as in Figures 1b–d.

One can see in Figure 3a that the periodic inversion and "phase transition" are not affected much by the dynamic potential, except for small oscillations of the beam profile. In the Fourier space (Figure 3b) and in the transformed frame (Figure 3c), the modulation coming from the dynamic potential becomes more pronounced.

Similar to the dynamic polynomial functions used in Figures 1 and 2, the trajectory of the beam in the Fourier space still obeys the dt/dz rule for the oscillating dynamic function, but now there are two oscillations present: one coming from the parabolic potential and the other coming from the oscillating dynamic function $t(z)$, as seen in the top panel. There is also the oscillation coming from dt/dz, visible in the middle panel, but that one is just the phase-shifted dynamic oscillation. The bottom panel clearly displays the two superposed oscillations. Here, we have chosen $b = 4$ to make the period $2\pi/b = \pi/2$ of the dynamic potential commensurate with the inversion period $2\pi/\alpha = 4\pi$. In the complete inversion period (both the first and second stages), there will be then eight oscillation periods, which can be seen from the middle and bottom panels in Figure 3. One may choose other values for the parameter b, and the results will remain similar. In comparison with the modulation mechanisms shown in Figures 1 and 2, the oscillating dynamic potential in Figure 3 exhibits more complex behavior, and therefore points to more possibilities for manipulating Airy beams by picking more varied dynamic potentials.

6. Two-dimensional Case

Last but not least, we extend the analysis to the 2D case. The Schrödinger-like equation that governs the propagation of the

© 2020 WILEY-VCH Verlag GmbH & Co. KGaA, Weinheim

beam can be written as

$$i\frac{\partial\psi(x,y,z)}{\partial z} = -\frac{1}{2}\left(\frac{\partial^2}{\partial x^2}+\frac{\partial^2}{\partial y^2}\right)\psi(x,y,z) + \frac{1}{2}\alpha^2\left\{[x-t_1(z)]^2+[y-t_2(z)]^2\right\}\psi(x,y,z) \tag{15}$$

Since this problem is linear, we may solve it by the separation of variables and write the solution of Equation (15) as $\psi(x,y,z) = X(x,z)Y(y,z)$, so that Equation (15) can be recast into

$$i\frac{\partial X}{\partial z}+\frac{1}{2}\frac{\partial^2 X}{\partial x^2}-\frac{1}{2}\alpha^2[x-t_1(z)]^2X-mX=0 \tag{16}$$

$$i\frac{\partial Y}{\partial z}+\frac{1}{2}\frac{\partial^2 Y}{\partial y^2}-\frac{1}{2}\alpha^2[y-t_2(z)]^2Y+mY=0 \tag{17}$$

in which m is the separation constant. If we introduce $X(x,z) = f(x,z)\exp(-imz)$ and $Y(y,z) = g(y,z)\exp(imz)$, Equations (16) and (17) can be rewritten as

$$i\frac{\partial f}{\partial z}+\frac{1}{2}\frac{\partial^2 f}{\partial x^2}-\frac{1}{2}\alpha^2[x-t_1(z)]^2f=0 \tag{18}$$

$$i\frac{\partial g}{\partial z}+\frac{1}{2}\frac{\partial^2 g}{\partial y^2}-\frac{1}{2}\alpha^2[y-t_2(z)]^2g=0 \tag{19}$$

which are two independent 1D cases, as described in Equation (1). As a result, the 2D case can be reduced to the product of two independent 1D cases, which makes the physical picture of the 2D case quite clear, and we do not discuss it further here.

7. Conclusion

Summarizing, we have investigated the propagation of Airy beams in dynamic parabolic potentials. In the polynomial dynamic parabolic potentials, the propagation trajectory of the Airy beams in the real space is determined by the dynamic potential, while in the Fourier space, the propagation trajectory is determined by the derivative of the dynamic potential. Likewise in the oscillating parabolic potentials, the propagation trajectory in real space is not affected much by the dynamic potential, but exhibits superposed oscillations. The dynamic parabolic potentials provide more varied manipulation possibilities for Airy beams, and therefore may broaden their potential applications.

Acknowledgements

This work was supported by the Natural Science Foundation of Shaanxi province (2017JZ019), Chinese Postdoctoral Science Foundation (2018M633499), Fundamental Research Funds for the Central Universities (xzy012019038, xzy022019076), and Qatar National Research Fund, project NPRP 11S-1126-170033. The authors acknowledge the computational resources provided by the HPC platform of Xi'an Jiaotong University. Some small errors in the names of the authors of this manuscript were corrected on April 9th, 2020, after online publication.

Conflict of Interest

The authors declare no conflict of interest.

Keywords

Airy beams, dynamic potentials, parabolic potentials

Received: December 11, 2019
Revised: February 9, 2020
Published online: March 16, 2020

[1] M. V. Berry, N. L. Balazs, *Am. J. Phys.* **1979**, *47*, 264.
[2] G. A. Siviloglou, D. N. Christodoulides, *Opt. Lett.* **2007**, *32*, 979.
[3] G. A. Siviloglou, J. Broky, A. Dogariu, D. N. Christodoulides, *Phys. Rev. Lett.* **2007**, *99*, 213901.
[4] J. Broky, G. A. Siviloglou, A. Dogariu, D. N. Christodoulides, *Opt. Express* **2008**, *16*, 12880.
[5] Y. Hu, G. A. Siviloglou, P. Zhang, N. K. Efremidis, D. N. Christodoulides, Z. Chen, in: *Nonlinear Photonics and Novel Optical Phenomena*, edited by Z. Chen and R. Morandotti, Springer Series in Optical Sciences Vol. 170 Springer, New York **2012**, pp. 1–46.
[6] M. A. Bandres, I. Kaminer, M. Mills, B. M. Rodriguez-Lara, E. Greenfield, M. Segev, D. N. Christodoulides, *Opt. Phot. News* **2013**, *24*, 30.
[7] Z. Zhang, Y. Hu, J. Y. Zhao, P. Zhang, Z. G. Chen, *Chin. Sci. Bull.* **2013**, *58*, 3513.
[8] N. K. Efremidis, Z. Chen, M. Segev, D. N. Christodoulides, *Optica* **2019**, *6*, 686.
[9] I. Kaminer, M. Segev, D. N. Christodoulides, *Phys. Rev. Lett.* **2011**, *106*, 213903.
[10] A. Lotti, D. Faccio, A. Couairon, D. G. Papazoglou, P. Panagiotopoulos, D. Abdollahpour, S. Tzortzakis, *Phys. Rev. A* **2011**, *84*, 021807.
[11] I. Dolev, I. Kaminer, A. Shapira, M. Segev, A. Arie, *Phys. Rev. Lett.* **2012**, *108*, 113903.
[12] Y. Q. Zhang, M. Belić, Z. K. Wu, H. B. Zheng, K. Q. Lu, Y. Y. Li, Y. P. Zhang, *Opt. Lett.* **2013**, *38*, 4585.
[13] Y. Q. Zhang, M. R. Belić, H. B. Zheng, H. X. Chen, C. B. Li, Y. Y. Li, Y. P. Zhang, *Opt. Express* **2014**, *22*, 7160.
[14] M. Shen, J. Gao, L. Ge, *Sci. Rep.* **2015**, *5*, 9814.
[15] F. Diebel, B. M. Bokić, D. V. Timotijević, D. M. J. Savić, C. Denz, *Opt. Express* **2015**, *23*, 24351.
[16] N. K. Efremidis, V. Paltoglou, W. von Klitzing, *Phys. Rev. A* **2013**, *87*, 043637.
[17] A. Salandrino, D. N. Christodoulides, *Opt. Lett.* **2010**, *35*, 2082.
[18] P. Zhang, S. Wang, Y. Liu, X. Yin, C. Lu, Z. Chen, X. Zhang, *Opt. Lett.* **2011**, *36*, 3191.
[19] A. Minovich, A. E. Klein, N. Janunts, T. Pertsch, D. N. Neshev, Y. S. Kivshar, *Phys. Rev. Lett.* **2011**, *107*, 116802.
[20] L. Li, T. Li, S. M. Wang, C. Zhang, S. N. Zhu, *Phys. Rev. Lett.* **2011**, *107*, 126804.
[21] Y. Hu, M. Li, D. Bongiovanni, M. Clerici, J. Yao, Z. Chen, J. Azaña, R. Morandotti, *Opt. Lett.* **2013**, *38*, 380.
[22] R. Driben, Y. Hu, Z. Chen, B. A. Malomed, R. Morandotti, *Opt. Lett.* **2013**, *38*, 2499.
[23] L. Zhang, K. Liu, H. Zhong, J. Zhang, Y. Li, D. Fan, *Opt. Express* **2015**, *23*, 2566.

© 2020 WILEY-VCH Verlag GmbH & Co. KGaA, Weinheim

[24] Y. Hu, A. Tehranchi, S. Wabnitz, R. Kashyap, Z. Chen, R. Morandotti, *Phys. Rev. Lett.* **2015**, *114*, 073901.
[25] M. A. Bandres, J. C. Gutiérrez-Vega, *Opt. Express* **2007**, *15*, 16719.
[26] Y. Q. Zhang, M. R. Belić, L. Zhang, W. P. Zhong, D. Y. Zhu, R. M. Wang, Y. P. Zhang, *Opt. Express* **2015**, *23*, 10467.
[27] Y. Q. Zhang, X. Liu, M. R. Belić, W. P. Zhong, M. S. Petrović, Y. P. Zhang, *Ann. Phys.* **2015**, *363*, 305.
[28] Y. Q. Zhang, X. Liu, M. R. Belić, W. P. Zhong, F. Wen, Y. P. Zhang, *Opt. Lett.* **2015**, *40*, 3786.
[29] Z. Pang, D. Deng, *Opt. Express* **2017**, *25*, 13635.
[30] W. Liu, D. N. Neshev, I. V. Shadrivov, A. E. Miroshnichenko, Y. S. Kivshar, *Opt. Lett.* **2011**, *36*, 1164.
[31] N. K. Efremidis, *Opt. Lett.* **2011**, *36*, 3006.
[32] H. Zhong, Y. Q. Zhang, M. R. Belić, C. B. Li, F. Wen, Z. Y. Zhang, Y. P. Zhang, *Opt. Express* **2016**, *24*, 7495.
[33] W. P. Zhong, M. R. Belić, T. Huang, *Optik* **2013**, *124*, 2397.
[34] A. W. Snyder, D. J. Mitchell, *Science* **1997**, *276*, 1538.
[35] U. Levy, S. Derevyanko, Y. Silberberg, *Prog. Opt.* **2016**, *61*, 237.
[36] Y. Q. Zhang, D. Zhang, Z. Y. Zhang, C. B. Li, Y. P. Zhang, F. L. Li, M. R. Belić, M. Xiao, *Optica* **2017**, *4*, 571.

© 2020 WILEY-VCH Verlag GmbH & Co. KGaA, Weinheim